Nitrous oxide production in autotrophic nitrogen removal granular sludge: A modeling study

Chen, Xueming; Ni, Bing-Jie; Sin, Gürkan

Published in:
Biotechnology and Bioengineering

Link to article, DOI:
10.1002/bit.26937

Publication date:
2019

Document Version
Peer reviewed version

Xueming Chen ORCID iD: 0000-0003-4009-9810

Gürkan Sin ORCID iD: 0000-0003-0513-4502

Nitrous Oxide Production in Autotrophic Nitrogen Removal Granular Sludge: A Modeling Study

Xueming Chen[1,*], Bing-Jie Ni[2,*], Gürkan Sin[1]

[1]Process and Systems Engineering Center (PROSYS), Department of Chemical and Biochemical Engineering, Technical University of Denmark, 2800 Kgs. Lyngby, Denmark

[2]Centre for Technology in Water and Wastewater, School of Civil and Environmental Engineering, University of Technology Sydney, Sydney, NSW 2007, Australia

***Corresponding authors:**

Dr. Xueming Chen, Phone: +45 8194 8080, E-mail: xuem.chen@hotmail.com

Dr. Bing-Jie Ni, Phone: +61 2 9514 7401, E-mail: bingjieni@gmail.com

ABSTRACT

The sustainability of autotrophic granular system performing partial nitration and anaerobic ammonium oxidation (Anammox) for complete nitrogen removal is impaired by the production of nitrous oxide (N_2O). A systematic analysis of the pathways and affecting parameters is therefore required for developing N_2O mitigation strategies. To this end, a mathematical model capable of describing different N_2O production pathways was defined in this work by synthesizing relevant mechanisms of ammonium-oxidizing bacteria (AOB), nitrite-oxidizing bacteria (NOB), heterotrophic bacteria (HB), and Anammox bacteria. With the model validity reliably tested and verified using two independent sets of experimental data from two different autotrophic nitrogen removal biofilm/granular systems, the defined model was applied to reveal the underlying mechanisms of N_2O production in the granular structure as well as the impacts of operating conditions on N_2O production. The results show that: 1) in the aerobic zone close to the granule surface where AOB contribute to N_2O production through both the AOB denitrification pathway and the NH_2OH pathway, the co-

This article has been accepted for publication and undergone full peer review but has not been through the copyediting, typesetting, pagination and proofreading process, which may lead to differences between this version and the Version of Record. Please cite this article as doi: 10.1002/bit.26937.

occurring HB consume N_2O produced by AOB but indirectly enhance the N_2O production through providing NO from NO_2^- reduction for the NH_2OH pathway, 2) the inner anoxic zone of granules with the dominance of Anammox bacteria acts as a sink for NO_2^- diffusing from the outer aerobic zone and therefore reduces N_2O production from the AOB denitrification pathway, 3) operating parameters including bulk DO, influent NH_4^+, and granule size affect the N_2O production in the granules mainly through regulating the NH_2OH pathway of AOB, accounting for 34%~58% of N_2O turnover, and 4) the competition between the NH_2OH pathway and heterotrophic denitrification for nitric oxide leads to the positive role of HB in reducing N_2O production in the autotrophic nitrogen removal granules, which could be further enhanced with the presence of a proper level of influent organics.

Graphical Abstract

The sustainability of autotrophic granular system performing partial nitration and anaerobic ammonium oxidation (Anammox) for complete nitrogen removal is impaired by the production of nitrous oxide (N_2O). A systematic analysis of the pathways and affecting parameters is therefore required for developing N_2O mitigation strategies.

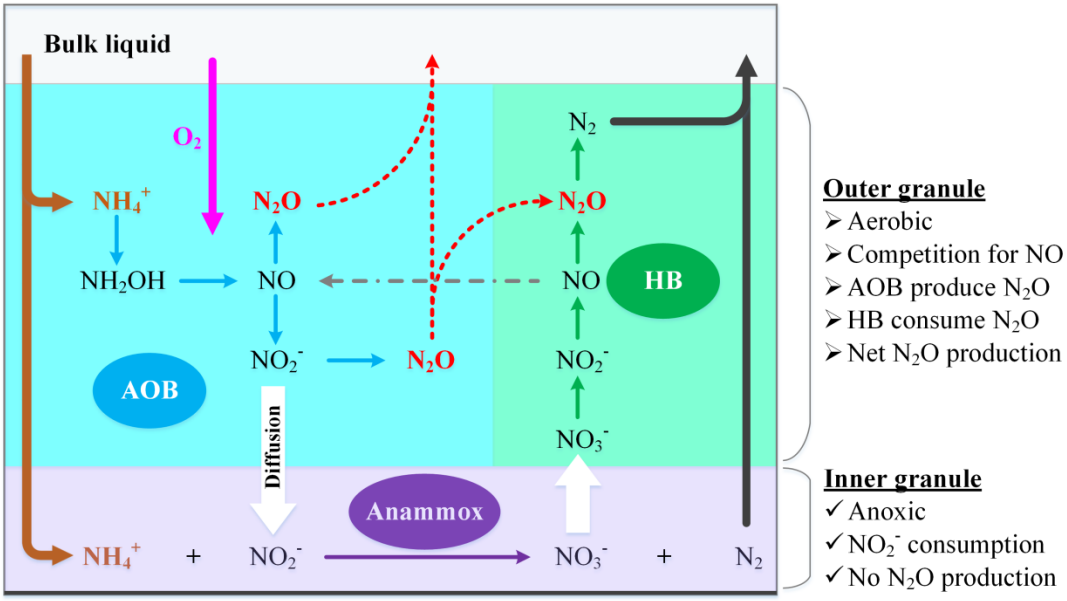

Keywords: Nitrous oxide (N_2O); granule; anaerobic ammonium oxidation (Anammox); partial nitritation; mathematical modeling

1. INTRODUCTION

Compared to the conventional nitrification and denitrification process, the autotrophic nitrogen removal through combining partial nitritation with anaerobic ammonium oxidation (Anammox) represents a more sustainable alternative due to its less requirement for aeration, lower production of sludge, and saving of organic carbon for energy recovery (Jetten et al.

2001; Kuenen 2008; Sliekers et al. 2002). An application survey by Lackner et al. (2014) reported over 100 full-scale installations worldwide performing partial nitriation/Anammox (PN/A), around 90% of which were operated as single-stage systems.

Nevertheless, studies have documented various N_2O emissions from PN/A systems of different scales (Ali et al. 2016; Castro-Barros et al. 2015; Domingo-Félez et al. 2014; Joss et al. 2009; Sliekers et al. 2002). N_2O is not only a potent greenhouse gas with a global warming effect 265 times stronger than carbon dioxide but also a major scavenger of stratospheric ozone leading to ozone layer depletion (IPCC 2014; Ravishankara et al. 2009). It is generally recognized that Anammox bacteria don't produce N_2O (Kartal et al. 2006); N_2O is therefore not specifically included in the stoichiometry of Anammox process. Thus, autotrophic nitrifiers, i.e., ammonium-oxidizing bacteria (AOB), have been regarded as the main contributors to the N_2O production in autotrophic PN/A systems through either the hydroxylamine (NH_2OH) pathway or the AOB denitrification pathway or both. Heterotrophic bacteria (HB) might grow on microbial decay products under inorganic influent conditions and therefore sustain in autotrophic nitrogen removal systems (Lotti et al. 2014; Mozumder et al. 2014; Ni et al. 2012). Despite the proposed positive contribution to nitrogen removal through reducing nitrate produced by Anammox bacteria, the presence of HB might also play a significant role in regulating the N_2O production in autotrophic nitrogen removal systems, as N_2O is an obligate intermediate of the sequential heterotrophic denitrification process (Hanaki et al. 1992).

Relative to biomass of suspended growth, compact sludge aggregates in the form of granules are particularly suitable to obtain the coexistence of AOB and Anammox bacteria in single-stage autotrophic nitrogen removal system. The DO concentration gradient in granules enables the creation of spatially separated aerobic and anoxic zones for AOB and Anammox bacteria, respectively. Moreover, the large accumulation of microbial decay products in the granular structure (Matsumoto et al. 2009) might be conducive to the proliferation of HB.

However, among the numerous studies reported so far, limited efforts have been dedicated to investigating the N_2O production in single-stage autotrophic granular systems. Ali et al. (2016) applied the isotopic composition analysis to identify the N_2O production pathways in a single-stage PN/A granular reactor. However, the relative contribution of HB denitrification to N_2O production could not be distinguished from that of the AOB denitrification pathway. The complicated interactions between different N_2O production pathways mediated by various microorganisms place the foremost difficulty in both qualitatively and quantitatively analyzing the N_2O production in autotrophic granular systems solely through experimentation.

Mathematical modeling can serve as a powerful tool for gaining an in-depth, microscale understanding of the rather complicated processes associated with N_2O production. Lu et al. (2018) extended the Activated Sludge Model No. 1 (ASM1) to decipher the N_2O production pathways in an autotrophic granular sequencing batch reactor. However, the usage of a homogeneous model that lumped granular structure into apparent substrate affinities might overlook the important role of granular structure characterized by substrate concentration gradients and microbial stratification in the underlying N_2O production mechanisms. In fact, previous model-based studies have revealed that the consideration of analogous biofilms as either suspended or attached growth in the model did generate distinctly different N_2O production characteristics for both nitrifying biofilms (Sabba et al. 2015) and denitrifying biofilms (Sabba et al. 2017). Although Van Hulle et al. (2012) applied a one-dimensional biofilm model to study the N_2O emissions during autotrophic nitrogen removal in a granular system, the NH_2OH pathway of AOB and the contribution of HB were overlooked. In view of the above, more efforts are still needed to systematically and comprehensively explore the N_2O productions in autotrophic nitrogen removal granular systems.

This work therefore aims to further understand the mechanisms of N_2O production in autotrophic nitrogen removal granules. To this end, a mathematical model capable of describing relevant mechanisms in autotrophic nitrogen removal systems was firstly defined.

The validity of the defined model was then tested and verified using two independent sets of literature reported experimental data; one was taken from an analogous autotrophic nitrogen removal biofilm reactor while the other from an enriched granular reactor. The verified model was coupled with relevant mass transfer terms in the modelling platform to simulate an autotrophic granular system in continuous mode. Extensive simulations were lastly performed to disclose the underlying mechanisms of N_2O formation and reduction inside the autotrophic granules as well as the impacts of operating conditions on the N_2O production and pathway differentiation in the autotrophic nitrogen removal granular system.

2. MATERIALS AND METHODS

2.1.Model Description

As presented in Fig. 1, the mathematical model in this work synthesizes relevant mechanisms of functional microorganisms in an autotrophic nitrogen removal system including AOB, nitrite oxidizing bacteria (NOB), HB, and Anammox bacteria. The detailed process reactions of AOB and HB as N_2O mediators are included in the supporting information (SI). The three pathways considered for N_2O production in this work include 1) N_2O as a by-product of incomplete oxidation of NH_2OH to NO_2^- via NO by AOB (i.e., the NH_2OH pathway), 2) N_2O as the final product of AOB denitrification (i.e., the AOB denitrification pathway), and 3) N_2O as an intermediate of sequential reduction of oxidized nitrogen oxides to N_2 by HB. In the defined model, NO reduction to N_2O in the NH_2OH pathway is coupled with NH_2OH oxidation to NO_2^-, while direct NO_2^- reduction to N_2O in the AOB denitrification pathway is accompanied by NH_2OH oxidation. This setup of AOB-associated N_2O production pathways is consistent with Pocquet et al. (2016) and has been proved capable of reliably describing and predicting N_2O production dynamics when AOB played a significant role (Ni et al. 2011; Ni et al. 2013; Pocquet et al. 2016).

To reduce the model complexity whilst maintaining the high model validity, ionized NH_4^+ and NO_2^- which could be directly and reliably measured (instead of unionized NH_3 and HNO_2) are assumed to be the substrate for AOB and NOB, respectively, in the model. In addition, the possible inhibition of NH_3 and HNO_2 on the activities of AOB and NOB are neglected, as their concentrations are usually relatively low compared to their inhibitory levels (Pocquet et al. 2016). However, similar to Chen et al. (2018) and Ni et al. (2011), the inhibition of DO on the AOB denitrification pathway is accounted for in the model. The aerobic reaction of NOB and the anoxic reaction of Anammox bacteria are described by following the generally accepted modelling practice. The Activated Sludge Model for Nitrogen (ASMN) (Hiatt and Grady 2008) is adopted to describe the mechanisms of HB, including the sequential denitrification from NO_3^- to NO_2^-, NO, N_2O and finally to N_2 under anoxic conditions and the anabolism for biomass growth under aerobic conditions. The decay process for each microbial species is modelled to generate inert and slowly biodegradable organics. The slowly biodegradable organics is subject to hydrolysis to yield readily biodegradable organics, thus making it possible for HB to grow in an autotrophic nitrogen removal system without external input of organics.

In summary, the defined model contains 9 soluble components and 6 solid components, as listed in Table S1 in the SI. The stoichiometric relationships of all components that conform to mass balance are presented in Table S2 (SI). Except for the decay processes which are represented by the first-order equation with respect to biomass, kinetic control of all microbial reactions, as shown in Table S3 (SI), is described by the Monod equation. The model parameters as well as their values, units, and sources are summarized in Table S4 (SI).

2.2.Experimental Data for Testing Model Validity

Two independent experimental datasets previously reported in Wang et al. (2017) and Lu et al. (2018) that studied N_2O production dynamics in autotrophic nitrogen removal

biofilm/granular systems under different operational conditions were used to test the validity of the defined model.

Dataset 1 (Wang et al. 2017): In order to obtain one-stage completely autotrophic nitrogen removal, Wang et al. (2017) applied a 15-L steady-state sequencing batch biofilm reactor (SBBR) with polyacrylonitrile-activity carbon fiber (PAN-ACF) to support the attached growth of biomass. The SBBR was fed with inorganic synthetic wastewater containing 200 g NH_4^+-N/m^3 and operated in 24-h cycles, consisting of 5-min feeding phase, 23-h reacting phase with aeration and mixing, 50-min settling phase, and 5-min decanting phase. The data for model testing captured bihourly variations of NH_4^+, NO_2^-, NO_3^-, and N_2O in the SBBR for 22 hours during a typical operational cycle with DO controlled at 2.00 ± 0.20 g/m^3. The applicability of these reported data for testing the defined model could be justified by the following two facts: 1) the operational data clearly demonstrated the SBBR's capability of achieving completely autotrophic nitrogen removal and 2) the microbial community analysis directly revealed the coexistence of AOB, NOB, HB, and Anammox bacteria in the biofilm (Wang et al. 2017).

Dataset 2 (Lu et al. 2018): The N_2O production behavior was observed in a 10-L bench-scale plexiglass sequencing batch reactor (SBR) with biomass retained in the form of granules. The SBR was fed with inorganic synthetic wastewater containing a mixture of 140 g NH_4^+-N/m^3 and 182 g NO_2^--N/m^3 and operated in 3-h cycles, consisting of 30-min feeding phase, 2-h mixing phase, 20-min settling phase, and 10-min decanting phase withdrawing an aliquot of 2.5 L. The data for model testing described the dynamic variations of NH_4^+, NO_2^-, NO_3^-, and N_2O in the SBR for the first 2.5 hours of an operational cycle as a batch test, the low DO of which was derived from atmospheric reoxygenation. The detected microbial diversity and the clearly documented activities of AOB, NOB, HB, and Anammox bacteria in the granules proved the applicability of these reported data for testing the defined model.

2.3.Model Testing and Simulation Approach

The same set of model parameters was used throughout to test the validity of the defined model as well as for all the following simulations. The SBBR was represented as a one-dimensional planar biofilm reactor compartment while the granular SBR was modelled as a one-dimensional spherical biofilm reactor compartment in AQUASIM (Reichert 1998). Following the practice proposed by Wanner and Morgenroth (2004), the stoichiometric and kinetic relationships between components of the defined model were constructed in the biofilm reactor compartment to simulate the autotrophic nitrogen removal with involvement of N_2O production mediated by the cohort of AOB, NOB, HB, and Anammox bacteria. Diffusion of soluble components in biofilm matrix was set with the introduction of reduced diffusion coefficients in water, which are provided in Table S5 (SI).

Model testing using Dataset 1 reported in Wang et al. (2017) was performed as a two-step process to verify the defined model. In the first step, the biofilm area was adjusted to fit the cycle data of NH_4^+, NO_2^-, and NO_3^- by assuming a biomass density of 100000 g-COD/m^3, a biofilm porosity of 0.75 (Koch et al. 2000), and an average biofilm thickness of 800 μm (Wang et al. 2017). The biomass composition was set according to the relative abundance of species in the microbial community analysis recorded in Wang et al. (2017), i.e., AOB of 7.77%, NOB of 6.91%, Anammox of 5.44%, and HB of 7.73%, with the remaining biomass (72.15%) being recognized as the sum of slowly biodegradable and inert organics. In the second step, instead of N_2O concentration, the accumulative N_2O production, indicative of total N_2O productivity, was compared with the N_2O predicted by the model configured in the first step without further adjustment. The reason for such a two-step model evaluation process was mainly due to the unavailability of direct measurement of biofilm dimensions, thus posing the foremost difficulty for the accurate representation of such a SBBR in the model. However, the validity of the defined model in terms of the intrinsic structure regulating the relationship between nitrogen removal capacity and N_2O production dynamics would still be

guaranteed, provided that a good match between experimental data and model prediction could be obtained simultaneously for both steps.

Model testing using Dataset 2 reported in Lu et al. (2018) was conducted by applying all NH_4^+, NO_2^-, NO_3^-, and N_2O profiles simultaneously to further verify the defined model. Assuming a biomass density of 100000 g-COD/m^3 and a biofilm porosity of 0.75 (Koch et al. 2000), the number of granules in the SBR was calculated based on the measured median granule size (D50 = 728 μm) and the mixed liquor volatile suspended solids (MLVSS) concentration (2399 g/m^3) reported in Lu et al. (2018). Similar to the aforementioned handling, the biomass composition was decided by reference to the experimentally quantified abundance of microbial species in consideration of slowly biodegradable and inert organics. Mass transfer of N_2O from the liquid phase of the SBR to the atmosphere was modelled through a gas-liquid mass transfer equation mediated by the mass transfer coefficient $K_L a$ and the Henry's law constant H (Schulthess and Gujer 1996), i.e., $R_{N2O} = K_L a_{N2O}(S_{N2O} - \frac{S_{N2O,air}}{H_{N2O}})$, where $K_L a_{N2O}$ was assumed at 2 d^{-1}, $S_{N2O,air}$ was 0.0003 g-N/m^3, and H_{N2O} was 1.9 (Foley et al. 2010). If a good agreement between experimental data and model prediction could still be achieved, the validity of the defined model would be regarded as high enough to reliably support the subsequent model-based evaluations.

2.4.Simulations for Revealing Mechanisms of N_2O Production and Its Affecting Factors

Different simulation scenarios (cf. Table S5 in the SI) were performed using the tested model to explore the N_2O production in an autotrophic nitrogen removal granular system, which was modelled to be operated in continuous mode and composed of spherical granules with a uniform size in AQUASIM (Reichert 1998). The base scenario (Scenario 0) probed into the mechanisms of N_2O formation and reduction in autotrophic nitrogen removal granules and assumed 1) an average granule size (radius) of 500 μm, 2) an influent NH_4^+ concentration of 500 g-N/ m^3, 3) a constant bulk DO concentration of 0.25 g/m^3, and 4) an influent COD

concentration of 0. Other 4 scenarios were then implemented to investigate the impacts of operating conditions on the N_2O production in the autotrophic granular system. Specifically, Scenarios 1 to 3 focused on bulk DO concentration of 0.10 – 0.50 g/m^3, influent NH_4^+ concentration of 50 – 1000 g-N/m^3, and granule size (radius) of 50 – 1000 μm, respectively. Considering that the potential existence of some biodegradable organics in wastewater might affect the growth of HB and therefore alter the overall microbial community structure, Scenario 4 was designed to assess the impact of influent organics concentration of 0 – 100 g-COD/m^3 on the autotrophic granular system.

For all simulation scenarios, a total system volume of 1 m^3 (including 0.2 m^3 of granules and 0.8 m^3 of bulk liquid) and an inflow rate of 1 m^3/d was considered, giving rise to a hydraulic retention time of 1 day. The number of granules was calculated by dividing the total volume of granules by the volume of each granule. Assuming the same biomass density and porosity as used in model testing, the total solid concentration in the autotrophic granular system was 5000 g-COD/m^3 for all simulation scenarios. The setting of diffusion of soluble components in the granular structure was in line with model testing, and zero-flux of soluble components was set at the granule center. Similar to Sabba et al. (2015), the mass transfer resistance through the liquid boundary layer was neglected for all soluble components; the concentration at the granule surface was equal to that in the bulk liquid. For the convenience of data calculation and the consistency in results interpretation, the N_2O produced was assumed to leave the continuously-operated autotrophic granular reactor in the effluent; no liquid-to-gas transfer of N_2O was considered in all the model simulations. This setting was acceptable in view of the essential N_2O production inside the granules and the minor impact of potential liquid-to-gas transfer of N_2O (in the form of a zero and non-zero mass transfer coefficient for N_2O) on the N_2O production factor (i.e., a relative change of < 5%) of the studied autotrophic granular system requiring a relatively low DO level, as demonstrated in Figure S1 in the SI.

For each simulation scenario, the initial concentrations of all 9 soluble components in the autotrophic granules as well as the bulk liquid were assumed to be zero, while each of AOB, NOB, HB, Anammox bacteria, and abiotic organics (inert organics (50%) + slowly biodegradable organics (50%)) was assumed to take up 20% of the initial solid COD in the granules. The steady-state granule size was controlled by the surface detachment velocity without considering re-attachment of detached solids. All simulations assumed an initial granule radius of 50 μm and were run to reach steady-state conditions indicated by constant effluent concentrations, N_2O production, granule size, and microbial composition.

3. RESULTS

3.1.Testing Model Predictive Capability with Experimental Data

At the first step of the model testing process using Dataset 1, the biofilm area was adjusted to 1.4 m^2, which rendered a good match (R^2=0.95) between the model predicted and experimentally measured data in terms of NH_4^+ consumption, NO_3^- formation, and NO_2^- accumulation, as illustrated in Fig. 2A. On top of the satisfactory result obtained at the first step, the defined model was able to predict the accumulative N_2O production during a typical operational cycle to a high degree (R^2=0.99) in the second step, as evidenced by Fig. 2B. A good performance was also acquired for model testing with Dataset 2 (Fig. 3). The defined model was able to capture not only the bulk transformations of NH_4^+, NO_3^-, and NO_2^- (R^2=0.92) in Fig. 3A but also the trace profile of N_2O (R^2=0.97) in the granular reactor. With these, the defined model has been proved capable of describing the relationship between nitrogen removal capacity and N_2O production dynamics in the autotrophic nitrogen removal biofilm/granular systems involving AOB, NOB, HB, and Anammox bacteria simultaneously. Therefore, the defined model could be reliably applied in the following simulations to assess N_2O production in the autotrophic granular system in a holistic manner.

3.2.Mechanisms of N_2O Production inside Autotrophic Granules

This section explores the mechanisms of N_2O production inside autotrophic granules under the conditions of Scenario 0 (Table S5 in the SI), which gives a total nitrogen (TN) removal efficiency (i.e., ratio between N_2 produced and influent NH_4^+) of 90.3% with an accompanying net N_2O production factor (i.e., ratio of net N_2O produced to total NH_4^+ removed) of 1.7%. Granule radius-wise profiles are presented in Fig. 4, where "r" denotes the rate of individual process listed in Table S3 (SI) while "R" indicates the net rate of certain soluble nitrogenous component taking into account all relevant processes that produce or consume it. A positive "R" means net production while a negative "R" represents net consumption.

Overall, steady-state microbial stratification (Fig. 4A) and substrate concentration gradients (Fig. 4B) are observed in the representative autotrophic granule. AOB and HB only exist at the granule surface, and their fractions decrease towards the interior of the granule from 500 μm to 400 μm. By comparison, the fraction of Anammox bacteria peaks at 400 μm and drops consistently towards both the granule core (0 μm) and the bulk liquid (500 μm). NOB are absent in the entire range of granule radius. Due to the efficient conversion of slowly biodegradable organics (X_S) by HB at the granule surface, X_S is not present between 400 μm and 500 μm, while inert organics (X_I) is immanent across the granule radius as a result of the persistent biomass decay processes. Different from the nearly constant concentrations of NO_3^-, NH_2OH, NO, and N_2O in the representative autotrophic granule, the profiles of soluble components in Fig. 4B clearly exhibit the decreasing trends of NH_4^+ and NO_2^- from the bulk liquid to the granule core and the quick consumption of DO at the granule surface from 500 μm to 400 μm, well in line with the profiles of AOB and HB in Fig. 4A.

As shown in Fig. 4C, the process rates of NH_4^+ oxidation to NH_2OH (r1), NH_2OH oxidation to NO (r2), NO oxidation to NO_2^- (r3), NO reduction to N_2O (r4), and NO_2^-

reduction to N_2O (r5) by AOB all exhibit decreasing trends in the granule from 500 μm to 400 μm. Similar to Sabba et al. (2015) investigating N_2O production from nitrifying biofilms, NH_2OH produced in the outer layer of the granule diffuses into the inner layer which serves as a sink for NH_2OH, making r2 exceed r1 therein. Consequently, NH_2OH is lost in the outer granule while there is gain of NH_2OH in the inner granule, as reflected in the positive net NH_2OH conversion rate (R_{NH2OH}^{AOB}) between 480 μm and 500 μm and the negative R_{NH2OH}^{AOB} between 400 μm and 480 μm (Fig. 4D). Both the NH_2OH pathway (r4) and the AOB denitrification pathway (r5) contribute to the steady-state N_2O production by AOB in the granule (i.e., R_{N2O}^{AOB} in Fig. 4D). Fig. 4E illustrates the process rates of aerobic growth (r6), anoxic NO_3^- reduction to NO_2^- (r7), anoxic NO_2^- reduction to NO (r8), anoxic NO reduction to N_2O (r9), and anoxic N_2O reduction to N_2 (r10) by HB in the representative granule. Compared to other processes, the significantly higher value of r6 indicates the usage of the majority of hydrolyzed biodegradable organics (S_S) as the substrate to sustain the aerobic growth instead of the anoxic denitrifying activities of HB. The slight shift of the maximum r7, r8, r9, and r10 from the granule surface at 500 μm where HB biomass is highest to the granule radius at 490 μm is due to the inhibition by DO that is maximum at the granule surface. Resulting from the competition between the NH_2OH pathway of AOB and HB denitrification for NO, the rate of anoxic NO reduction to N_2O (r9) is much lower than r8 and r10 (Fig. 4E), leading to the positive net NO conversion rate (R_{NO}^{HB}) and the negative net N_2O conversion rate (R_{N2O}^{HB}) in the granule (Fig. 4F). The process rates of NO_2^- reduction (r11) and NH_4^+ oxidation (r12) by Anammox bacteria in Fig. 4G follow the same distribution pattern of Anammox bacteria in the representative granule (Fig. 4A). The inexistence of NOB throughout the granule radius corresponds to the null process rate of NO_2^- oxidation by NOB (r13), as shown in Fig. 4G.

The collective contributions of AOB, NOB, HB, and Anammox bacteria to the conversion rates of NH_4^+ (R_{NH4}), NO_2^- (R_{NO2}), NO_3^- (R_{NO3}), NH_2OH (R_{NH2OH}), NO (R_{NO}),

and N_2O (R_{N2O}) are displayed in Fig. 4H. N_2O production only takes place at the granule surface between 400 μm and 500 μm. Both HB and Anammox bacteria exert direct and/or indirect impact on N_2O production in the granule. The low consumption of NO_2^- by HB in the granule (i.e., the slightly negative R_{NO2}^{HB} in Fig. 4F) manifests the negligible impact of HB on the AOB denitrification pathway for N_2O production (i.e., r5 in Fig. 4C), which is dependent on the availability of NO_2^-. Since R_{NO} in Fig. 4H is around 0, the net NO production by HB (i.e., the positive R_{NO}^{HB} in Fig. 4F) is compensated by the net NO consumption by AOB (i.e., the negative R_{NO}^{AOB} in Fig. 4D). Therefore, the NO produced by HB is mainly directed to favor the N_2O production by AOB through the NH_2OH pathway (i.e., r4 in Fig. 4C). In this sense, HB play an indirect role in affecting the NH_2OH pathway of AOB for N_2O production in the autotrophic granule. Moreover, the direct consumption of N_2O by HB (i.e., the negative R_{N2O}^{HB} in Fig. 4F) results in the lower overall R_{N2O} (Fig. 4H) than the net N_2O production rate of AOB (i.e., R_{N2O}^{AOB} in Fig. 4D). As the influent is lacking in NO_2^-, Anammox bacteria gain access to NO_2^- produced by AOB through its diffusion from the outer granule to the inner granule. The NO_2^- consumption by Anammox bacteria in the inner granule not only facilitates the autotrophic nitrogen removal but also lowers the availability of NO_2^- for N_2O production through the AOB denitrification pathway (i.e., r5 in Fig. 4C). The relatively high conversion rates of NH_4^+ and NO_2^- as shown in Fig. 4H give rise to the stratification of NH_4^+ and NO_2^- inside the autotrophic granule, whereas the nearly even distribution of NO_3^-, NH_2OH, NO, and N_2O in Fig. 4B is mainly determined by their diffusivities in presence of relatively low conversion rates.

3.3.Impacts of Operating Parameters on N_2O production in Autotrophic Granule

This section examines the effects of bulk DO concentration (Scenario 1), influent NH_4^+ concentration (Scenario 2), granule size (radius) (Scenario 3), and influent organics concentration (Scenario 4) on the N_2O production in the autotrophic nitrogen removal

granular system. To this end, steady-state TN removal efficiency is correlated with the corresponding microbial community structure in the granules, while steady-state net N_2O production factor is analyzed in reference to the accompanying contribution differentiation of N_2O production pathways. The simulated results are compiled in Fig. 5.

3.3.1. Impact of bulk DO

Nitrogen removal. As shown in Fig. 5A, a low bulk DO of 0.10 g/m^3 limits oxygen supply for AOB to oxidize influent NH_4^+ to NO_2^- for Anammox bacteria; most NH_4^+ is left untreated in the effluent. As a result, a low TN removal efficiency of 34.1% is mediated by AOB (7.3%), HB (2.2%), and Anammox bacteria (90.5%) in the granules. The increase in bulk DO to 0.20 g/m^3 enhances partial nitritation by AOB, thus creating more NO_2^- for Anammox bacteria. Therefore, the active biomass fraction of Anammox bacteria increases to 91.1% while that of AOB remains around 7.3%. The active biomass fraction of HB drops to 1.5% due to their simultaneous competitions with AOB and Anammox bacteria for oxygen and NO_2^-, respectively. The resulting TN removal efficiency reaches 86.4% at bulk DO of 0.20 g/m^3 (Fig. 5A). A higher bulk DO of around 0.25 g/m^3 leads to nearly complete utilization of influent NH_4^+ and intensifies the competition between AOB and Anammox bacteria for the influent NH_4^+ supply. Consequently, the active biomass fraction of AOB drops to 6.8% while that of Anammox bacteria and HB increases to 91.3% and 1.9%, respectively, giving rise to the peak TN removal efficiency of 90.3% (Fig. 5A). Further increase in bulk DO to the maximum studied in this work (i.e., 0.50 g/m^3) pushes AOB towards full nitritation and generates an unbalanced, excessive NO_2^-/NH_4^+ ratio for Anammox bacteria. In consequence, as depicted in Fig. 5A, the active biomass fraction of Anammox bacteria decreases while those of AOB and HB increase, leading to the descending TN removal efficiency.

N_2O production. The increasing N_2O production factor from 1.5% at bulk DO of 0.10 g/m^3 to 2.5% at bulk DO of 0.20 g/m^3 (Fig. 5B) is in line with the increasing activity of AOB

in NH_4^+ oxidation. Further increase in bulk DO firstly causes an abrupt drop of N_2O production factor to 1.7% at bulk DO of 0.25 g/m^3 and then leads to the gradual decrease in N_2O production factor, which reaches 1.3% at bulk DO of 0.50 g/m^3. As indicated in Fig. 5B, the increase in bulk DO from 0.10 g/m^3 to 0.20 g/m^3 motivates N_2O production from both the AOB denitrification pathway and the NH_2OH pathway while diminishing the contribution of HB denitrification. Further increase in bulk DO till 0.50 g/m^3 brings no significant change to the contribution of the AOB denitrification pathway. By contrast, the positive contribution (i.e., production) of the NH_2OH pathway decreases consistently, compensated by the increasing negative contribution (i.e., consumption) of HB denitrification to N_2O turnover (Fig. 5B).

3.3.2. Impact of influent NH_4^+

Nitrogen removal. A too low influent NH_4^+ concentration represents limited NH_4^+ supply for Anammox bacteria to react with NO_2^- produced by AOB while a too high NH_4^+ concentration brings about insufficient NO_2^- production by AOB for Anammox bacteria to oxidize NH_4^+. Therefore, as demonstrated in Fig. 5C, an increasing influent NH_4^+ concentration from 50 g-N/m^3 to 200 g-N/m^3 increases the active biomass fraction of Anammox bacteria whilst decreasing those of AOB and HB, thus elevating the TN removal efficiency. At the influent NH_4^+ concentration of 300 g-N/m^3, the TN removal efficiency reaches the peak of 90.6% with AOB (6.0%), HB (2.0%), and Anammox bacteria (92.0%) coexisting in the granules. Further increase in the influent NH_4^+ concentration till 800 g-N/m^3 slightly promotes the active biomass fraction of AOB but demotes those of HB and Anammox bacteria in the granules. Despite the relatively stable abundance of AOB (7.1%), HB (1.7%), and Anammox bacteria (91.2%) in the granules at the influent NH_4^+ concentration of higher than 800 g-N/m^3, a downward trend is still observed for the TN removal efficiency in Fig. 5C.

N_2O production. At the influent NH_4^+ concentration of lower than 300 g-N/m^3, N_2O production factor is low and fluctuates around 1.0%, with the AOB denitrification pathway, the NH_2OH pathway, and HB denitrification each accounting for around 30%, 35%, and -35% of N_2O turnover (Fig. 5D). At the influent NH_4^+ concentration of 300 g-N/m^3 where maximum TN removal efficiency of 90.6% is obtained, the N_2O production factor is minimum with a value of 0.9%. An influent NH_4^+ concentration higher than 300 g-N/m^3 favors the NH_2OH pathway while suppressing the contribution of HB denitrification to N_2O turnover. By comparison, the significant increase in the influent NH_4^+ concentration from 300 g-N/m^3 to 1000 g-N/m^3 only gives rise to slight decrease in the contribution of the AOB denitrification pathway to N_2O turnover from 27.5% to 26.1% (Fig. 5D).

3.3.3. Impact of granule size

Nitrogen removal. A small granule radius of not higher than 100 μm enables oxygen penetration and therefore fails to create anoxic zone for Anammox bacteria, resulting in the dominance of AOB (~80%) and HB (~20%) in the granules and the trace TN removal (~1.3%) (Fig. 5E). When the granule radius is 200 μm, Anammox bacteria appear in the granules and cooperate with AOB and HB for nitrogen removal, corresponding to the TN removal efficiency of 35.6%. Granules with greater radius firstly increase and then decrease the TN removal efficiency, with the maximum value of 90.3% obtained at the granule radius of 500 μm (Fig. 5E). The increasing TN removal efficiency from 200 μm to 500 μm is because of the higher abundance of Anammox bacteria in the granules. In contrast, the decreasing TN removal efficiency when the granule radius exceeds 500 μm is the result of the limitation of NO_2^- diffusing from the surface to the inner layer of the granules, which pushes Anammox bacteria away from the granule core and makes the inner layer of the granules inactive. Therefore, with the increasing granule radius from 500 μm to 1000 μm, the active biomass fractions of AOB and HB gradually increase while that of Anammox bacteria slightly decreases, as described in Fig. 5E.

N_2O production. The increasing N_2O production factor from 1.0% to 1.5% when the granule radius increases from 50 μm to 100 μm is ascribed to the lowered negative contribution of HB denitrification to N_2O turnover (Fig. 5F), on top of the trace nitrogen removal performance due to the absence of Anammox bacteria. With the increasing presence of Anammox bacteria and the decreasing relative abundance of AOB and HB in the granules, the N_2O production factor slightly increases from 1.5% at the granule radius of 200 μm to 1.7% at the granule radius of 500 μm. Regarding N_2O turnover, the contribution of the NH_2OH pathway increases while those of the AOB denitrification pathway and HB denitrification decrease. Further increase in the granule radius to 1000 μm firstly leads to the enhanced NH_2OH pathway and then favors the N_2O consumption by HB. As a result, the N_2O production factor approaches the maximum of 2.5% at the granule radius of around 700 μm and is subject to insignificant change thereafter (Fig. 5F).

3.3.4. Impact of influent organics

Nitrogen removal. Different from the aforementioned simulated results of Scenarios 1 to 3, the granular system exhibits a much simpler trend when facing the influent organics (Scenario 4). As shown in Fig. 5G, the increasing organics in the influent stimulates the growth of HB in the granules and favors the heterotrophic denitrification process. Consequently, despite the decreasing abundance of AOB and Anammox bacteria, the TN removal increases slightly but consistently from 90.3% to 92.0% with the influent organics concentration within the studied range from 0 to 100 g-COD/m^3.

N_2O production. The simulated results in Fig. 5H clearly indicate the positive role of the influent organics in reducing the N_2O production in the granular system. With the increase in the influent organics concentration from 0 to 100 g-COD/m^3, the N_2O production factor drops consistently from 1.7% to 0.2%. Both the contributions of the AOB denitrification pathway

and the NH_2OH pathway to N_2O turnover decrease, while the N_2O consumption by HB is reinforced.

4. DISCUSSION

A better understanding of the pathways and affecting parameters formulates the basis for the development of reliable N_2O mitigation strategies for the single-stage autotrophic nitrogen removal granular system. Steady-state simulated results in Fig. 4A demonstrate clear microbial distribution in the granules. Similar trends have been documented in both experimental (Ali et al. 2016) and simulation studies (Liu et al. 2017; Mozumder et al. 2014) on granule-based systems for autotrophic nitrogen removal. The accompanying concentration profiles of soluble components in the granules (Fig. 4B) are consistent with previous experimental measurements (Ali et al. 2016; Nielsen et al. 2005; Vázquez-Padín et al. 2010; Wang et al. 2017) and simulated results (Liu et al. 2017). The distinct concentration gradients of DO, NH_4^+, and NO_2^- are due to their relatively high conversion rates in the granules (Fig. 4H), whereas the nearly even distribution of NO_3^-, NH_2OH, NO, and N_2O across the granule radius is regulated by their diffusivities in presence of relatively low conversion rates (Fig. 4H). On this basis, this work systematically explores the mechanisms of N_2O production inside the autotrophic granules with the spatially separated aerobic and anoxic zones. Firstly, N_2O production is shown to only take place in the aerobic zone at the granule surface, with simultaneous contributions of both the AOB denitrification pathway and the NH_2OH pathway. Secondly, though favoring the in-situ consumption of N_2O produced by AOB, the co-occurrence of HB in the aerobic zone is found to generate NO and thus indirectly enhance the N_2O production by AOB through the NH_2OH pathway. The fact that both AOB and HB are located close to the granule surface facilitates the diffusion of N_2O from the granules into the bulk liquid. Therefore, the autotrophic granular system in this work might produce more N_2O than the membrane-aerated biofilm system with counter diffusing fluxes of oxygen and ammonium, where N_2O production has been shown to take place at the biofilm base (Ni and

Yuan 2013). Thirdly, the inner anoxic zone is discovered to act as a sink for NO_2^- diffusing from the outer aerobic zone and therefore reduce N_2O production through the AOB denitrification pathway. The multispecies nature of autotrophic granule complicates the mechanisms associated with N_2O production, which are significantly different from those reported for single-species nitrifying biofilms (Sabba et al. 2015) and denitrifying biofilms (Sabba et al. 2017).

Analyses on the impacts of operating parameters in Fig. 5 manifest the possibility of achieving high-level nitrogen removal whilst mitigating N_2O production in the granular system by 1) controlling bulk DO, influent NH_4^+, and granule size at proper levels, or 2) providing organic influent. NOB will be washed out of the granules due to their simultaneous competitions with AOB for oxygen and/or with HB and Anammox bacteria for nitrite. Consistent with Hao et al. (2002) and Liu et al. (2017), the increase in bulk DO firstly increases the aerobic ammonium oxidation and then inhibits the activity of Anammox bacteria (Fig. 5A). On the contrary, the increasing influent NH_4^+ concentration firstly improves the nitrogen removal by enhancing the Anammox process and then impedes the nitrogen removal because of limited oxygen supply (Fig. 5C). A too small granule size fails to provide the anoxic zone for Anammox bacteria while a too big granule size reduces the active biomass volume due to diffusion limitation in the granules (Fig. 5E). A proper level of influent organics benefits the nitrogen removal through enhancing the heterotrophic denitrification process present in the granules (Fig. 5G).

The N_2O production factor obtained in this work (0.2%-2.7%) is well in the range for single-stage autotrophic nitrogen removal systems reported Ali et al. (2016). Through analyzing the correlation between the contribution of each N_2O production pathway and the N_2O production factor under inorganic influent conditions (Scenarios 1, 2, and 3), it is found that the trends of N_2O production factor in Figs. 4B, 4D, and 4F are mainly mediated by the NH_2OH pathway considering its highest positive contribution to N_2O turnover (34%~58%)

and its highest correlation coefficient of >0.95 with the N_2O production factor. The AOB denitrification pathway also contributes significantly to N_2O production and accounts for 17%~31% of N_2O turnover. The HB denitrification consistently helps consume N_2O produced by AOB under the simulated conditions in this work. This is due to the competition between the NH_2OH pathway and HB denitrification for intermediate NO, which makes the N_2O formation rate from NO lower than the N_2O reduction rate by HB. The close interaction between the NH_2OH pathway and HB denitrification in regulating N_2O production is proved by their high correlation (i.e., 0.78 for Scenario 1 and 0.99 for Scenarios 2 and 3) as well as the very low NO concentration in the representative granule in Fig. 4B. Despite the minor role in affecting the nitrogen removal (Mozumder et al. 2014), HB growing on microbial decay products have been shown in this work to contribute significantly to reducing N_2O production in the autotrophic granular system. As shown in Fig. 5H, the positive role of HB in mitigating N_2O production will be enhanced by introducing a proper amount of organics in the influent, which therefore lowers the contributions of the AOB related pathways. From the perspective of practical application, the organics, if not already present in the influent wastewater, could originate from external addition to the granular system.

5. CONCLUSIONS

This work investigated the underlying mechanisms of N_2O production as well as the impacts of operating conditions on N_2O production in autotrophic nitrogen removal granules. The main conclusions are:

- In the aerobic zone close to the granule surface where AOB contribute to N_2O production through both the AOB denitrification pathway and the NH_2OH pathway, the co-occurring HB consume N_2O produced by AOB but indirectly enhance the N_2O production through the NH_2OH pathway.

- The inner anoxic zone of granules with the dominance of Anammox bacteria acts as a sink for NO_2^- diffusing from the outer aerobic zone and therefore reduces N_2O production from the AOB denitrification pathway.
- Operating parameters including bulk DO, influent NH_4^+, and granule size affect the N_2O production in the granules mainly through regulating the NH_2OH pathway of AOB, accounting for 34%~58% of N_2O turnover.
- The competition between the NH_2OH pathway and heterotrophic denitrification for nitric oxide leads to the positive role of HB in reducing N_2O production in the autotrophic nitrogen removal granules, which could be further enhanced with the presence of a proper level of influent organics.

ACKNOWLEDGEMENTS

Dr. Xueming Chen acknowledges the financial support by the European Union's Horizon 2020 research and innovation programme through Marie Skłodowska-Curie Individual Fellowship under grant agreement No. 790231. Dr. Bing-Jie Ni acknowledges the Australian Research Council (ARC) through Future Fellowship FT160100195.

CONFLICT OF INTEREST DISCLOSURE

The authors declare no conflict of interest.

REFERENCES

Ali M, Rathnayake RMLD, Zhang L, Ishii S, Kindaichi T, Satoh H, Toyoda S, Yoshida N, Okabe S. 2016. Source identification of nitrous oxide emission pathways from a single-stage nitritation-anammox granular reactor. Water Research 102:147-157.

Castro-Barros CM, Daelman MRJ, Mampaey KE, van Loosdrecht MCM, Volcke EIP. 2015. Effect of aeration regime on N2O emission from partial nitritation-anammox in a full-scale granular sludge reactor. Water Research 68:793-803.

Chen X, Yuan Z, Ni B-J. 2018. Nitrite accumulation inside sludge flocs significantly influencing nitrous oxide production by ammonium-oxidizing bacteria. Water Research 143:99-108.

Domingo-Félez C, Mutlu AG, Jensen MM, Smets BF. 2014. Aeration strategies to mitigate nitrous oxide emissions from single-stage nitritation/anammox reactors. Environmental Science & Technology.

Foley J, de Haas D, Yuan Z, Lant P. 2010. Nitrous oxide generation in full-scale biological nutrient removal wastewater treatment plants. Water Research 44(3):831-844.

Hanaki K, Hong Z, Matsuo T. 1992. Production of Nitrous Oxide Gas during Denitrification of Wastewater. Water Science and Technology 26(5-6):1027-1036.

Hao X, Heijnen JJ, van Loosdrecht MCM. 2002. Sensitivity analysis of a biofilm model describing a one-stage completely autotrophic nitrogen removal (CANON) process. Biotechnology and Bioengineering 77(3):266-277.

Hiatt WC, Grady CPL. 2008. An Updated Process Model for Carbon Oxidation, Nitrification, and Denitrification. Water Environment Research 80(11):2145-2156.

IPCC. 2014. Climate Change 2014: Synthesis Report. Contribution of Working Groups I, II and III to the Fifth Assessment Report of the Intergovernmental Panel on Climate Change. IPCC, Geneva, Switzerland. 151 p.

Jetten MSM, Wagner M, Fuerst J, van Loosdrecht M, Kuenen G, Strous M. 2001. Microbiology and application of the anaerobic ammonium oxidation (‘anammox’) process. Current Opinion in Biotechnology 12(3):283-288.

Joss A, Salzgeber D, Eugster J, Konig R, Rottermann K, Burger S, Fabijan P, Leumann S, Mohn J, Siegrist H. 2009. Full-Scale Nitrogen Removal from Digester Liquid with Partial Nitritation and Anammox in One SBR. Environmental Science & Technology 43(14):5301-5306.

Kartal B, Kuypers Marcel MM, Lavik G, Schalk J, Op den Camp Huub JM, Jetten Mike SM, Strous M. 2006. Anammox bacteria disguised as denitrifiers: nitrate reduction to dinitrogen gas via nitrite and ammonium. Environmental Microbiology 9(3):635-642.

Koch G, Egli K, Van der Meer JR, Siegrist H. 2000. Mathematical modeling of autotrophic denitrification in a nitrifying biofilm of a rotating biological contactor. Water Science and Technology 41(4-5):191-198.

Kuenen JG. 2008. Anammox bacteria: from discovery to application. Nature Reviews Microbiology 6(4):320-326.

Lackner S, Gilbert EM, Vlaeminck SE, Joss A, Horn H, van Loosdrecht MCM. 2014. Full-scale partial nitritation/anammox experiences – An application survey. Water Research 55(0):292-303.

Liu T, Ma B, Chen X, Ni B-J, Peng Y, Guo J. 2017. Evaluation of mainstream nitrogen removal by simultaneous partial nitrification, anammox and denitrification (SNAD) process in a granule-based reactor. Chemical Engineering Journal 327:973-981.

Lotti T, Kleerebezem R, Hu Z, Kartal B, Jetten MSM, van Loosdrecht MCM. 2014. Simultaneous partial nitritation and anammox at low temperature with granular sludge. Water Research 66(0):111-121.

Lu X, D. S. Pereira T, Al-Hazmi HE, Majtacz J, Zhou Q, Xie L, Makinia J. 2018. Model-Based Evaluation of N2O Production Pathways in the Anammox-Enriched Granular Sludge Cultivated in a Sequencing Batch Reactor. Environmental Science & Technology.

Matsumoto S, Katoku M, Saeki G, Terada A, Aoi Y, Tsuneda S, Picioreanu C, Van Loosdrecht Mark CM. 2009. Microbial community structure in autotrophic nitrifying granules characterized by experimental and simulation analyses. Environmental Microbiology 12(1):192-206.

Mozumder MSI, Picioreanu C, van Loosdrecht MCM, Volcke EIP. 2014. Effect of heterotrophic growth on autotrophic nitrogen removal in a granular sludge reactor. Environmental Technology 35(8):1027-1037.

Ni B-J, Ruscalleda M, Smets BF. 2012. Evaluation on the microbial interactions of anaerobic ammonium oxidizers and heterotrophs in Anammox biofilm. Water Research 46(15):4645-4652.

Ni BJ, Ruscalleda M, Pellicer-Nacher C, Smets BF. 2011. Modeling Nitrous Oxide Production during Biological Nitrogen Removal via Nitrification and Denitrification: Extensions to the General ASM Models. Environmental Science & Technology 45(18):7768-7776.

Ni BJ, Ye L, Law YY, Byers C, Yuan ZG. 2013. Mathematical Modeling of Nitrous Oxide (N2O) Emissions from Full-Scale Wastewater Treatment Plants. Environmental Science & Technology 47(14):7795-7803.

Ni BJ, Yuan ZG. 2013. A model-based assessment of nitric oxide and nitrous oxide production in membrane-aerated autotrophic nitrogen removal biofilm systems. Journal of Membrane Science 428:163-171.

Nielsen M, Bollmann A, Sliekers O, Jetten M, Schmid M, Strous M, Schmidt I, Larsen LH, Nielsen LP, Revsbech NP. 2005. Kinetics, diffusional limitation and microscale distribution of chemistry and organisms in a CANON reactor. FEMS Microbiology Ecology 51(2):247-256.

Pocquet M, Wu Z, Queinnec I, Spérandio M. 2016. A two pathway model for N2O emissions by ammonium oxidizing bacteria supported by the NO/N2O variation. Water Research 88(Supplement C):948-959.

Ravishankara AR, Daniel JS, Portmann RW. 2009. Nitrous Oxide (N2O): The Dominant Ozone-Depleting Substance Emitted in the 21st Century. Science 326(5949):123-125.

Reichert P. 1998. AQUASIM 2.0-Computer program for the identification and simulation of aquatic systems. EAWAG, Dubendorf, Switzerland.

Sabba F, Picioreanu C, Nerenberg R. 2017. Mechanisms of nitrous oxide (N2O) formation and reduction in denitrifying biofilms. Biotechnology and Bioengineering 114(12):2753-2761.

Sabba F, Picioreanu C, Pérez J, Nerenberg R. 2015. Hydroxylamine Diffusion Can Enhance N2O Emissions in Nitrifying Biofilms: A Modeling Study. Environmental Science & Technology 49(3):1486-1494.

Schulthess RV, Gujer W. 1996. Release of nitrous oxide (N2O) from denitrifying activated sludge: Verification and application of a mathematical model. Water Research 30(3):521-530.

Sliekers AO, Derwort N, Gomez JLC, Strous M, Kuenen JG, Jetten MSM. 2002. Completely autotrophic nitrogen removal over nitrite in one single reactor. Water Research 36(10):2475-2482.

Van Hulle SWH, Callens J, Mampaey KE, van Loosdrecht MCM, Volcke EIP. 2012. N2O and NO emissions during autotrophic nitrogen removal in a granular sludge reactor – a simulation study. Environmental Technology 33(20):2281-2290.

Vázquez-Padín J, Mosquera-Corral A, Campos JL, Méndez R, Revsbech NP. 2010. Microbial community distribution and activity dynamics of granular biomass in a CANON reactor. Water Research 44(15):4359-4370.

Wang X-X, Fang F, Chen Y-P, Guo J-S, Li K, Wang H. 2017. N2O micro-profiles in biofilm from a one-stage autotrophic nitrogen removal system by microelectrode. Chemosphere 175:482-489.

Wanner O, Morgenroth E. 2004. Biofilm modeling with AQUASIM. Water science and technology 49(11):137.

Figures

Fig. 1. Schematic of the model for autotrophic nitrogen removal involving the mechanisms of AOB, NOB, HB, and Anammox bacteria.

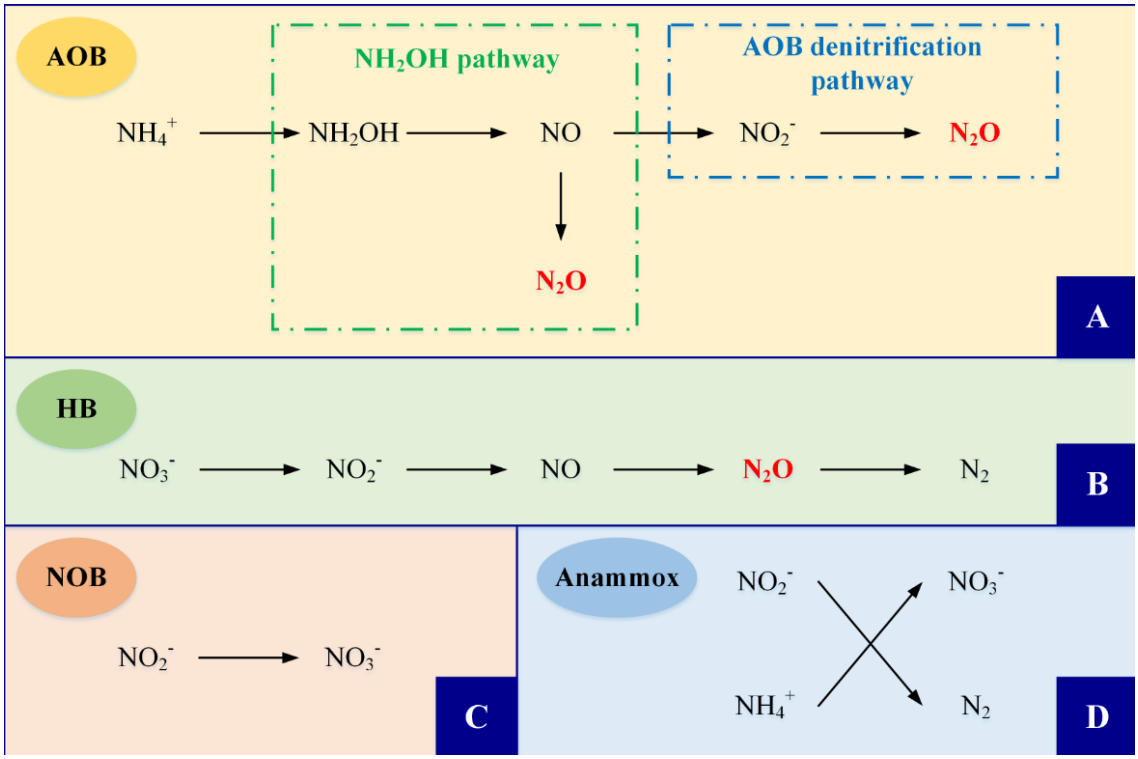

Fig. 2. Model evaluation results based on experimental cycle data of **(A)** NH_4^+, NO_2^- and NO_3^-, and **(B)** N_2O reported in Wang et al. (2017).

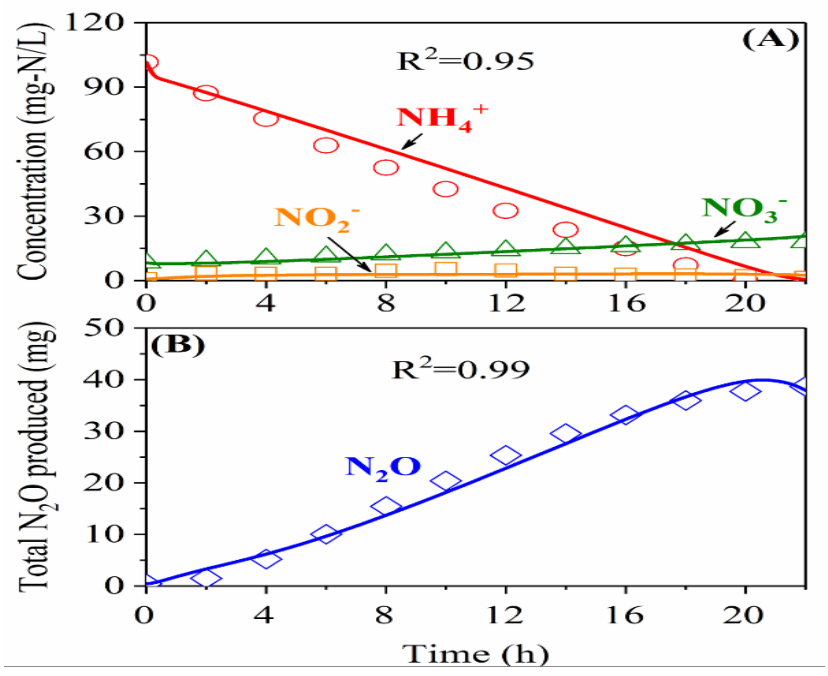

Fig. 3. Model evaluation results based on experimental batch data of **(A)** NH_4^+, NO_2^- and NO_3^-, and **(B)** N_2O reported in Lu et al. (2018).

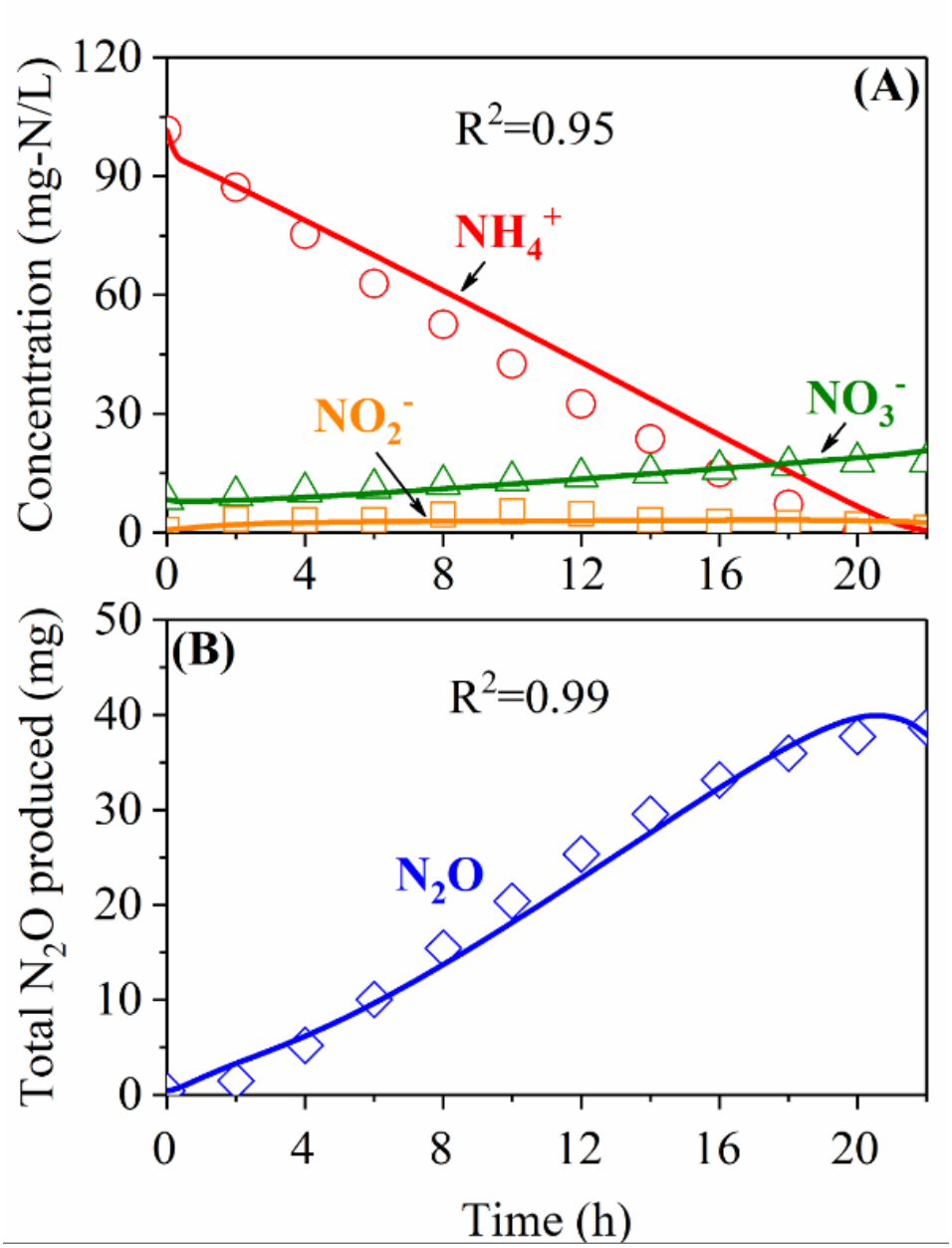

Fig. 4. Profiles of component fractions/concentrations and process/conversion rates in a representative granule: **(A)** active particulate components, **(B)** soluble components, **(C)** process rates of AOB, **(D)** conversion rates of nitrogenous components by AOB, **(E)** process rates of HB, **(F)** conversion rates of nitrogenous components by HB, **(G)** process rates of Anammox and NOB, and **(H)** overall conversion rates of nitrogenous components.

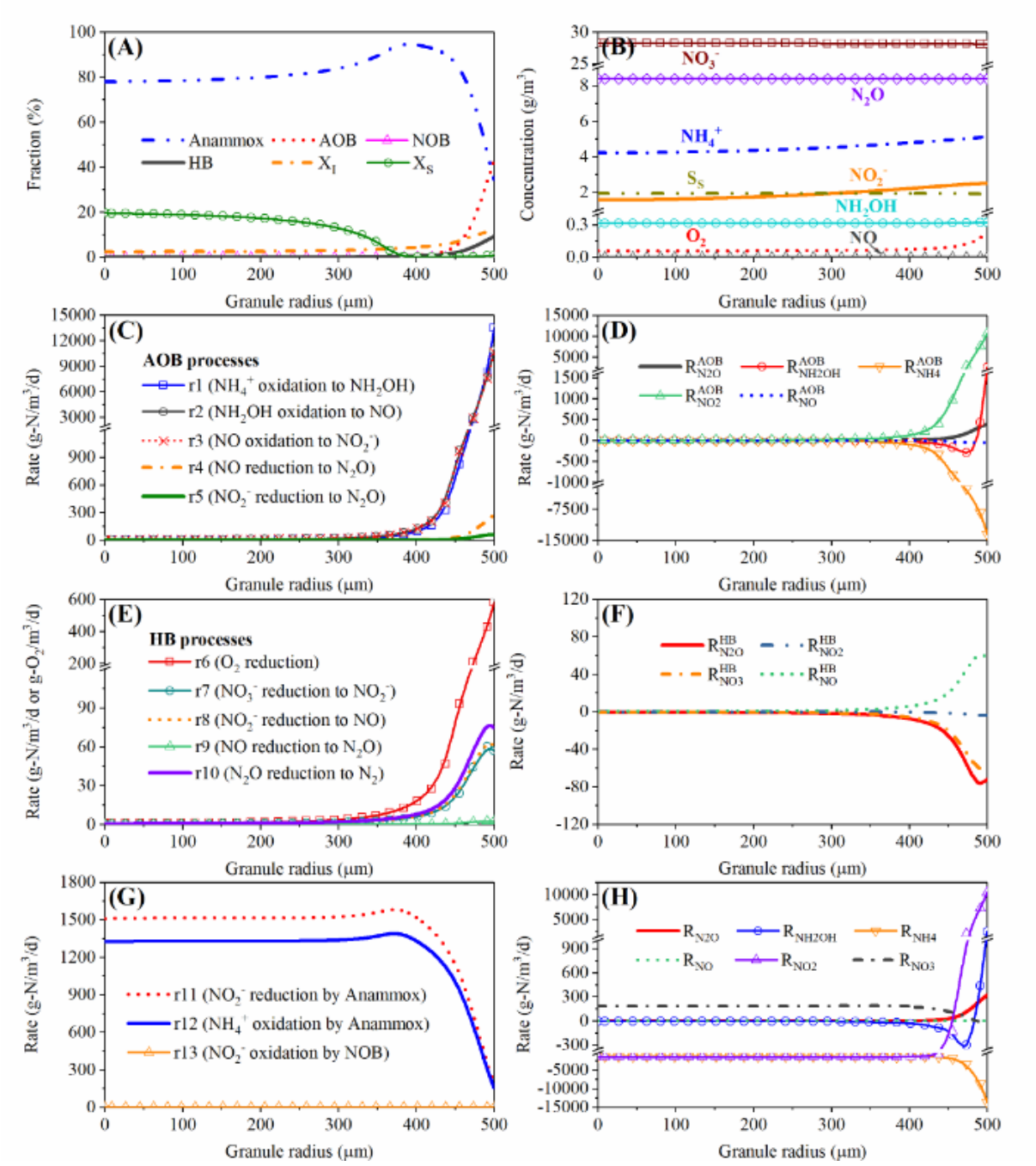

Fig. 5. Effects of **(A** and **B)** bulk DO, **(C** and **D)** influent NH_4^+, **(E** and **F)** granule size, and **(G** and **H)** influent organics on active biomass fraction and TN removal performance as well as net N_2O production factor and contribution differentiation of N_2O production pathways.